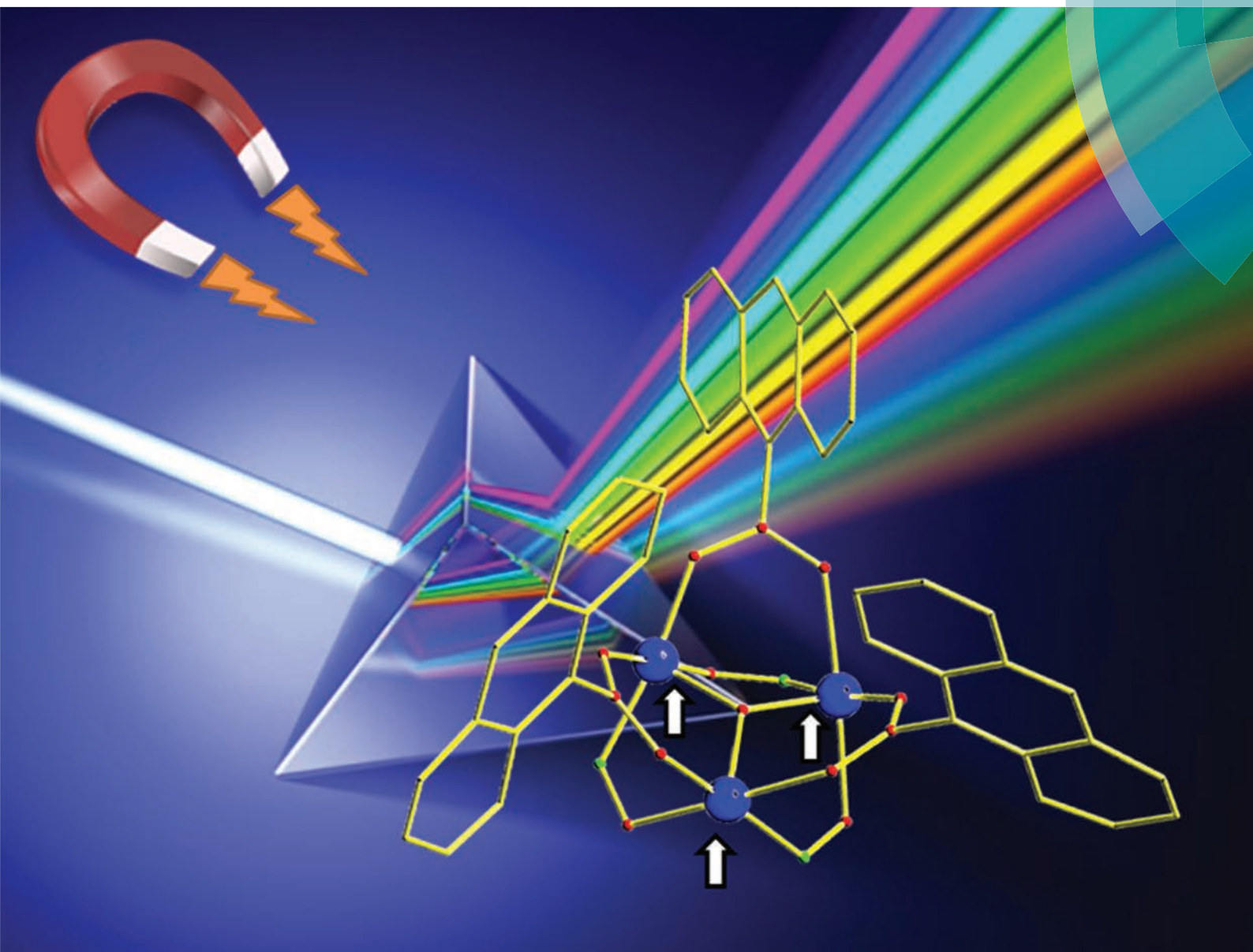


# Dalton Transactions

An international journal of inorganic chemistry

[www.rsc.org/dalton](http://www.rsc.org/dalton)



ISSN 1477-9226



**COVER ARTICLE**

Stamatatos *et al.*

Emissive molecular nanomagnets: introducing optical properties in triangular oximate {Mn<sup>III</sup><sub>3</sub>} SMMs from the deliberate replacement of simple carboxylate ligands with their fluorescent analogues

# Emissive molecular nanomagnets: introducing optical properties in triangular oximato {Mn<sup>III</sup><sub>3</sub>} SMMs from the deliberate replacement of simple carboxylate ligands with their fluorescent analogues†

Cite this: *Dalton Trans.*, 2014, **43**, 1965

Received 26th September 2013,  
Accepted 2nd November 2013

DOI: 10.1039/c3dt52571f

www.rsc.org/dalton

Dimitris I. Alexandropoulos,<sup>a</sup> Andrew M. Mowson,<sup>b</sup> Melanie Pilkington,<sup>a</sup>  
Vlasoula Bekiri,<sup>c</sup> George Christou<sup>b</sup> and Theocharis C. Stamatatos\*<sup>a</sup>

**The targeted replacement of acetate groups in the optically inactive [Mn<sup>III</sup><sub>3</sub>O(O<sub>2</sub>CMe)<sub>3</sub>(mpko)<sub>3</sub>(ClO<sub>4</sub>) single-molecule magnet with their naphthalene, anthracene, and pyrene fluorescent analogues has led to three new emissive SMMs with enhanced photoluminescence properties and potential applications in the field of molecular electronics.**

Magnetic materials find widespread utility in numerous areas of a modern society, from sensors, switches, speakers, and computer hard-drives, to medical and daily applications such as magnetic resonance imaging and cooling processes, respectively.<sup>1</sup> Miniaturization of magnetism-based devices is a major technological imperative, and thus a bottom-up molecular source of nanosized magnets would be invaluable.<sup>2</sup> In fact, exactly this became available in the early 1990s when it was discovered that individual molecules can function as magnets, and these were named single-molecule magnets (SMMs).<sup>3</sup> SMMs are magnetically interacting species with a significant ground state spin value, *S*, and an easy-axis-type magnetic anisotropy (*D*).<sup>3,4</sup> Such molecules often have a significant energy barrier to reversal of the magnetization (magnetic moment) vector, and thus at sufficiently low temperatures they function as nanoscale magnetic particles.<sup>4</sup> In addition, they can display quantum effects such as quantum tunneling of the magnetization (QTM) and quantum phase interference.<sup>5</sup> These represent a proof-of-feasibility, and a significant challenge for

the future is to build on this foundation and prepare SMMs that operate at higher temperatures (*i.e.*, liquid N<sub>2</sub> temperature)<sup>6</sup> and/or are better tailored to applications within devices.<sup>7</sup>

Molecular electronics is undoubtedly an exciting area of research which promises to deliver new technology and modern devices to society.<sup>8</sup> It is based on the construction and fabrication of molecular species with intriguing magnetic properties, pronounced stability and robustness, and capability to be deposited on electrical conducting surfaces.<sup>9</sup> Furthermore, in order to gain access into some real applications for these species, such as molecular spintronics,<sup>10</sup> transistors<sup>11</sup> and spin valves,<sup>12</sup> we need to combine their magnetic properties with one or more additional properties, such as conductivity, chirality and luminescence. Owing to important perspectives in fundamental science and applications in nanotechnology or molecular electronics, these 'hybrid' (or multifunctional) molecular materials are the subject of considerable efforts which involve coexistence, interplay or synergy between the multiple physical properties.<sup>13</sup>

Toward this end, various attempts have been made to study SMMs at the single-molecule level by depositing them on different surfaces and investigating their conducting behavior, an experiment of vital importance in the field of molecular electronics.<sup>14</sup> However, problems related to the determination of the molecules' exact positions and dispersion on the surfaces usually render assignments and conclusions inaccurate and superficial. In principle, when SMMs are coupled with photoluminescence properties, it may be possible to precisely detect the positions of molecules on surfaces, and thus open a new perspective in the field of molecule-based electronics.<sup>15</sup> The self-assembly synthesis of such emissive SMMs has been limited to the use of lanthanide ions in complexes with various organic bridging ligands.<sup>16</sup> This is reasonable given the anisotropic and high-spin nature of many 4f-metal ions,<sup>17</sup> as well as their intense metal-centered emission when they are accompanied by appropriate antenna ligands.<sup>18</sup> However,

<sup>a</sup>Department of Chemistry, 500 Glenridge Ave, Brock University, L2S 3A1 St. Catharines, Ontario, Canada. E-mail: tstatamatos@brocku.ca

<sup>b</sup>Department of Chemistry, University of Florida, Gainesville, Florida 32611-7200, USA

<sup>c</sup>Department of Aquaculture and Fisheries Management, Technological Educational Institute of Messolonghi, 30 200 Messolonghi, Greece

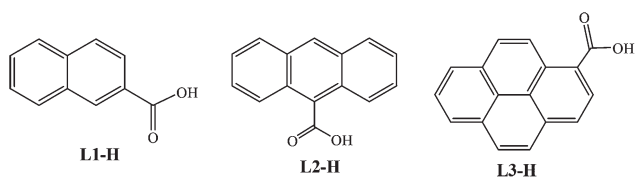
†Electronic supplementary information (ESI) available: Crystallographic data (CIF format), synthetic details, and various structural, magnetism and photoluminescence figures for complexes 2–4. CCDC 955993 and 955994. For ESI and crystallographic data in CIF or other electronic format see DOI: 10.1039/c3dt52571f

direct effect of the latter organic groups in the light emission of the SMM is totally unpredictable and of dubious origin. Hendrickson and coworkers have reported the only example of a photoluminescence 3d-metal SMM, a  $\{\text{Mn}^{\text{II}}\text{Mn}^{\text{III}}\}_2$  cluster from the self-assembly amalgamation of the optically inactive *N*-methyldiethanolamine and anthracenecarboxylic acid.<sup>15</sup>

In the absence of any previous studies on the *designed synthesis* of emissive, transition metal-based SMMs we decided to begin a program aiming at the deliberate replacement of non-emissive organic ligands in known SMMs with their fluorescent analogues, without affecting the metal-core structure and SMM properties. Undoubtedly, this is a difficult task considering that the new fluorescence ligands might alter the nuclearity of the compound, change the spin ground state and/or 'switch-off' the SMM property. Furthermore, the resulting photoluminescence induced by the fluorescence ligands could be quenched by the highly paramagnetic nature of the complex<sup>19</sup> leading to species with eventually no emitting behavior.

Taking all these possible obstacles into account, we undertook the challenge of performing carboxylate substitution reactions in the known, ferromagnetic triangular  $[\text{Mn}^{\text{III}}_3\text{O}(\text{O}_2\text{CMe})_3(\text{mpko})_3](\text{ClO}_4)$  (**1**) SMM (mpko<sup>-</sup> is the anion of methyl 2-pyridyl ketone oxime) with an  $S = 6$  ground state.<sup>20</sup> The carboxylic acids chosen (Scheme 1) were based on naphthalene, anthracene and pyrene, all organic substituents with simple fluorophores but with numerous applications in optics.<sup>21</sup> Thus, the representative reaction of **1** with an excess of 2-naphthoic acid (L1-H) in  $\text{CH}_2\text{Cl}_2$  afforded a dark brown solution. The solvent was removed *in vacuo*, toluene was added to the residue, and the solution was again evaporated to dryness. The addition and removal of toluene was repeated two more times. The remaining solid was redissolved in MeOH-THF and the resulting solution was layered with Et<sub>2</sub>O to afford dark purple crystals of  $[\text{Mn}^{\text{III}}_3\text{O}(\text{L1})_3(\text{mpko})_3](\text{ClO}_4)$  (**2**) in 95% yield.<sup>22</sup> The corresponding reactions with 9-anthracenecarboxylic acid (L2-H) and 1-pyrenecarboxylic acid (L3-H) gave the isostructural compounds  $[\text{Mn}^{\text{III}}_3\text{O}(\text{L2})_3(\text{mpko})_3](\text{ClO}_4)$  (**3**) and  $[\text{Mn}^{\text{III}}_3\text{O}(\text{L3})_3(\text{mpko})_3](\text{ClO}_4)$  (**4**) in 83 and 92% yields,<sup>22</sup> respectively. The complete removal of MeCO<sub>2</sub>H as its toluene azeotrope is essential for driving the equilibrium to the right and it guarantees the purity and high yield synthesis of the new products.<sup>23</sup>

The structures of the cations of **2** and **3** are very similar to that of the SMM precursor **1** (Fig. 1), and thus only the structure of representative complex **2** will be briefly described.



**Scheme 1** The fluorescent carboxylate ligands employed in the synthesis of complexes **2–4**.

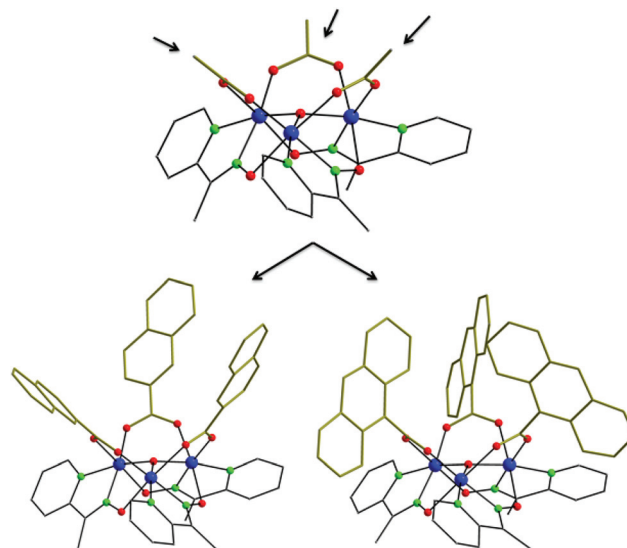


**Fig. 1** Molecular structures of the cations present in complexes **1** (top), **2** (bottom, left) and **3** (bottom, right), with the gold thick bonds emphasizing the different carboxylate moieties. Color scheme: Mn<sup>III</sup> blue, O red, N green, C gray. H-atoms are omitted for clarity.

The  $[\text{Mn}_3\text{O}(\text{L1})_3(\text{mpko})_3]^+$  cation of **2** consists of three Mn<sup>III</sup> atoms in a triangular arrangement bridged by a central  $\mu_3$ -oxido atom O1. Each edge of the Mn<sub>3</sub> triangle is bridged by an  $\eta^1:\eta^1:\mu\text{-L1}^-$  ion and an  $\eta^1:\eta^1:\eta^1:\mu\text{-mpko}^-$  ligand, with the pyridyl and oximate N atoms chelating a Mn<sup>III</sup> atom, forming a five-membered chelate ring. The Mn...Mn separations are almost equal (3.218–3.226 Å); the triangle is thus almost equilateral within the usual  $3\sigma$  criterion. The oxidation states of all Mn atoms were established as +3 by charge balance considerations and bond valence sum (BVS) calculations (Table S1†). The three L1<sup>-</sup> groups lie on one side of the Mn<sub>3</sub> plane, and the three oximate groups on the other. The Mn atoms are near-octahedral, and the Mn<sup>III</sup> centers exhibit a Jahn–Teller (JT) distortion, as expected for a high-spin d<sup>4</sup> ion in this geometry. The JT axes in both **2** and **3** involve the carboxylate and oximate O atoms, and are pointed outwards from the Mn<sub>3</sub> 'hard'-plane, thus contributing to the appearance of a significant molecular easy-axis anisotropy.<sup>20</sup> The central oxido atoms in **2** and **3** are 0.316 and 0.282 Å above the Mn<sub>3</sub> plane, respectively, on the same side as the carboxylate groups. These values are within the same range reported for **1**, and other similar triangles.<sup>20</sup> The average Mn–N–O–Mn torsion angles in **2** and **3** are 12.7 and 12.0°, respectively, slightly larger than that of 11.2° for **1**. Finally, as can be expected due to the existence of many aromatic rings in the carboxylate moieties of **2** and **3**, there are significant intermolecular  $\pi$ – $\pi$  stacking interactions which serve to link neighboring Mn<sub>3</sub> clusters in the crystal (Fig. S1†).

With respect to the magnetostructural correlations in the family of  $[\text{Mn}^{\text{III}}_3\text{O}(\text{O}_2\text{CR})_3(\text{mpko})_3]^+$  (R = various) triangles, it is now established that both the displacement of the central  $\mu_3$ -O<sup>2-</sup> out of the Mn<sub>3</sub> plane and the 'twisting' of the Mn–N–O–Mn units (as reflected in the corresponding torsion angles)

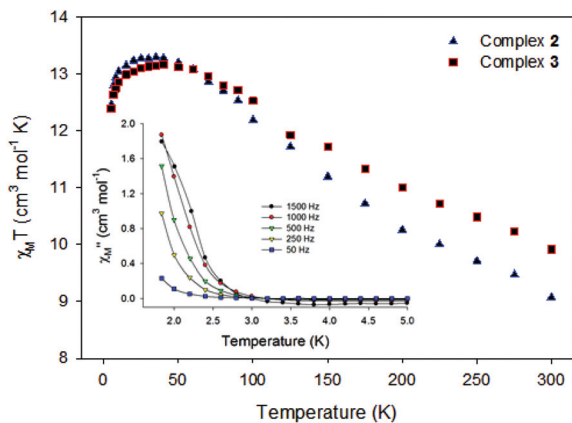


Fig. 2  $\chi_M T$  versus  $T$  plots of **2** and **3** in a 1 kG field. Inset: plot of the out-of-phase ( $\chi''_M$ ) ac susceptibility signals of complex **2** in a 3.5 G field oscillating at the indicated frequencies.

contribute to the weakening of the antiferromagnetic contribution and thus the observation of an overall ferromagnetic behavior.<sup>20,24</sup> This is also the case for the three new triangles **2**–**4**. For the sake of brevity, the magnetic properties of representative complexes **2** and **3** will be discussed.

Variable-temperature dc magnetic susceptibility measurements were performed on dried samples of **2** and **3** in the temperature range 5.0–300 K in an applied field of 1 kG (0.1 T). The data are shown as  $\chi_M T$  versus  $T$  plots in Fig. 2. The  $\chi_M T$  for **2** increases from  $9.08 \text{ cm}^3 \text{ mol}^{-1} \text{ K}$  at 300 K to a maximum of  $13.29 \text{ cm}^3 \text{ mol}^{-1} \text{ K}$  at 35.0 K and then decreases to  $12.47 \text{ cm}^3 \text{ mol}^{-1} \text{ K}$  at 5.0 K. Complex **3** exhibits similar behavior, with  $\chi_M T$  increasing from  $9.91 \text{ cm}^3 \text{ mol}^{-1} \text{ K}$  at 300 K to a maximum of  $13.17 \text{ cm}^3 \text{ mol}^{-1} \text{ K}$  at 40.0 K, and then decreasing to  $12.39 \text{ cm}^3 \text{ mol}^{-1} \text{ K}$  at 5.0 K. The 300 K values for **2** and **3** are slightly larger than the spin-only ( $g = 2$ ) value of  $9 \text{ cm}^3 \text{ mol}^{-1} \text{ K}$  for three non-interacting  $\text{Mn}^{\text{III}}$  ions. The shape of the curves indicates dominant ferromagnetic exchange interactions between the  $3\text{Mn}^{\text{III}}$  atoms corresponding to an  $S = 6$  ground state. However, the maxima for the two complexes, located at high temperature, are much below the spin-only value expected for a compound with a well-isolated  $S = 6$  ground state ( $21.00 \text{ cm}^3 \text{ mol}^{-1} \text{ K}$ ,  $g = 2$ ). This, combined with the simultaneous decrease in the  $\chi_M T$  values at high temperatures (>35 K), is likely due to the strong intermolecular antiferromagnetic exchange interactions and thermal population of excited states with  $S < 6$ . Attempts were made to fit the data to the theoretical expression for a  $3\text{Mn}^{\text{III}}$  isosceles triangle, but this approach was unfeasible due to the combined presence of strong intermolecular interactions, low-lying excited states (a direct result of the weak magnetic coupling), and crystal structure disorder.<sup>25</sup> The latter are also the reason for the unsuccessful fitting of the  $M/N\mu_B$  versus  $H/T$  data at low temperature, assuming that the ground state is solely populated.† Ac magnetic susceptibility studies were also performed on **2** and **3**, in a 3.5 G ac field oscillating at various frequencies and  $T < 15$  K. Below 3 K, the appearance of a frequency-dependent decrease in the in-phase signal ( $\chi'_M T$ , Fig. S2†) and a

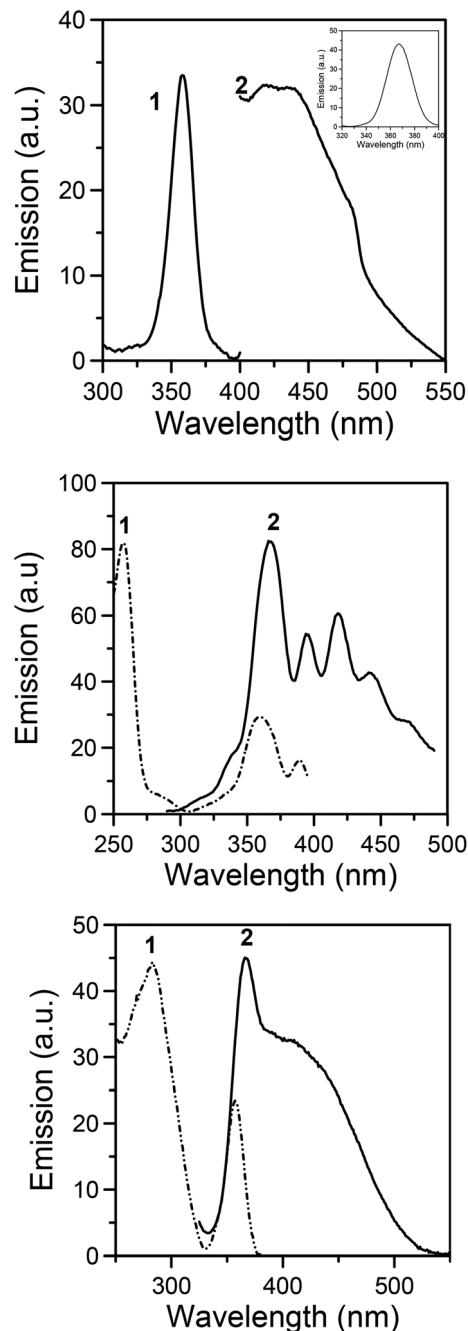


Fig. 3 Excitation (1) and emission (2) spectra of solid complexes **2** (top), **3** (middle), and **4** (bottom) at room temperature. Inset: the additional emission peak at 367 nm upon excitation at 270 nm.

concomitant increase in the out-of-phase ( $\chi''_M$ ) signal (inset of Fig. 2 and Fig. S3†) were suggestive of the superparamagnet-like slow relaxation of an SMM. The  $\chi''_M$  peak maxima for both compounds clearly lie at  $T < 1.8$  K, the operating limit of our SQUID magnetometer, and are located at the same  $T$  range and have the same strength with **1**.<sup>20</sup>

The photoluminescence properties of solids **1**–**4** were studied at room temperature. The free mpkoH ligand shows emission at 450 nm upon maximum excitation at 360 nm

(Fig. S4†). However, the  $[\text{Mn}^{\text{III}}_3\text{O}(\text{O}_2\text{CMe})_3(\text{mpko})_3](\text{ClO}_4)$  (**1**) SMM shows no emission in the entire visible region. This is likely due to a significant quenching of the emission intensity for **1** due to paramagnetic effects. In contrast, complexes **2–4** exhibit photoluminescence emission at room temperature (Fig. 3). In the case of complex **2**, two different characteristic emission areas are detected. The first band appears upon maximum excitation at 360 nm, and is obviously due to the mpkoH ligand, while the second with a maximum at 367 nm (upon UV excitation) is located in the same area where the naphthalene ligand emits.<sup>26</sup> Complexes **3** and **4** show a blue-shifted emission upon excitation at the UV-region, exhibiting the characteristic peaks of anthracene- and pyrene-units, respectively.<sup>26</sup> Interestingly, for complex **4** we observe both the monomer (peak at 370 nm) and the excimer (peak at 430 nm) emission of pyrene.<sup>26</sup>

## Conclusions

We have shown that it is indeed feasible to synthesize ‘hybrid’ molecular materials, and particularly emissive SMMs, through the deliberate replacement of non-emissive carboxylate groups with various fluorescence analogues without perturbing the structural core and the SMM property. The combined results demonstrate the beauty of molecular chemistry and the ability to manipulate physical properties in a targeted way, contributing to the development of advanced materials with implications in the field of molecular electronics. We are currently trying to (i) extend this route to many other emissive SMMs based on 3d-metals, (ii) perform low-temperature photomagnetic studies in order to ‘communicate’ the photoluminescence with the SMM property, (iii) perform single-crystal magnetic hysteresis studies in the presence of light, and (iv) deposit the reported compounds on a variety of conducting surfaces and evaluate the retention of their dual properties.

## Acknowledgements

We thank Ontario Trillium Foundation (graduate scholarship to D.I.A.), NSERC Discovery Grant (Th.C.S. and M.P.), CRC and CFI (M.P.), and National Science Foundation (DMR-1213030 to G.C.) for funding. V.B. acknowledges financial support by the European Union (European Social Fund – ESF) and Greek national funds through the Operational Program “Education and Lifelong Learning” of the National Strategic Reference Framework (NSRF) – Research Funding Program: Archimedes III.

## Notes and references

1 J. P. Liu, E. Fullerton, O. Gutfleisch and D. J. Sellmyer, *Nanoscale Magnetic Materials and Applications*, Springer, 2009.

- V. Balzani, M. Venturi and A. Credi, *Molecular Devices and Machines*, Wiley, 2003.
- (a) H.-J. Eppley, H.-L. Tsai, N. de Vries, K. Folting, G. Christou and D. N. Hendrickson, *J. Am. Chem. Soc.*, 1995, **117**, 301; (b) G. Christou, D. Gatteschi, D. N. Hendrickson and R. Sessoli, *MRS Bull.*, 2000, **25**, 66.
- (a) D. Gatteschi and R. Sessoli, *Angew. Chem., Int. Ed.*, 2003, **42**, 268; (b) G. Aromi and E. K. Brechin, *Struct. Bonding*, 2006, **122**, 1.
- (a) L. Thomas, L. Lioni, R. Ballou, D. Gatteschi, R. Sessoli and B. Barbara, *Nature*, 1996, **383**, 145; (b) W. Wernsdorfer and R. Sessoli, *Science*, 2000, 2417; (c) W. Wernsdorfer, N. E. Chakov and G. Christou, *Phys. Rev. Lett.*, 2005, **95**, 037203.
- J. D. Rinehart, M. Fang, W. J. Evans and J. R. Long, *J. Am. Chem. Soc.*, 2011, **133**, 14236.
- M. Mannini, F. Pineider, P. Sainctavit, C. Danieli, E. Otero, C. Sciancalepore, A. M. Talarico, M.-A. Arrio, A. Cornia, D. Gatteschi and R. Sessoli, *Nat. Mater.*, 2009, **8**, 194.
- E. Coronado, J. R. Galán-Mascarós, A. Murcia-Martínez, F. M. Romero and A. Tarazón, *Organic Conductors, Superconductors and Magnets: From Synthesis to Molecular Electronics*, NATO ASI Series, ed. L. Ouahab, E. Yagubskii, Kluwer Academic Publishers, 2004, vol. 139, pp. 127–142.
- (a) A. R. Rocha, V. M. García-suárez, S. W. Bailey, C. J. Lambert, J. Ferrer and S. Sanvito, *Nat. Mater.*, 2005, **4**, 335; (b) M. del Carmen Giménez-López, F. Moro, A. La Torre, C. J. Gómez-García, P. D. Brown, J. van Slageren and A. N. Khlobystov, *Nature Commun.*, 2011, **407**, 1415.
- L. Bogani and W. Wernsdorfer, *Nat. Mater.*, 2008, **7**, 179.
- R. Vincent, S. Klyatskaya, M. Ruben, W. Wernsdorfer and F. Balestro, *Nature*, 2012, **488**, 357.
- M. Urdampilleta, S. Klyatskaya, J.-P. Cleuziou, M. Ruben and W. Wernsdorfer, *Nat. Mater.*, 2011, **10**, 502.
- (a) L. Ouahab, *Multifunctional Molecular Materials*, Pan Stanford Publishing Pte. Ltd, 2013; (b) M. Morimoto, H. Miyasaka, M. Yamashita and M. Irie, *J. Am. Chem. Soc.*, 2009, **131**, 9823.
- (a) M. H. Jo, J. E. Grose, K. Baheti, M. M. Deshmukh, J. J. Sokol, E. M. Rumberger, D. N. Hendrickson, J. R. Long, H. Park and D. C. Ralph, *Nano Lett.*, 2006, **6**, 2014; (b) E. Coronado, C. Martí-Gastaldo and S. Tatay, *Appl. Surf. Sci.*, 2007, **254**, 225; (c) A. N. Abdi, J. P. Bucher, P. Rabu, O. Toulemonde, M. Drillon and P. J. Gerbier, *Appl. Phys.*, 2004, **95**, 7345.
- C. C. Beedle, C. J. Stephenson, K. J. Heroux, W. Wernsdorfer and D. N. Hendrickson, *Inorg. Chem.*, 2008, **47**, 10798.
- (a) M.-E. Boulon, G. Cucinotta, J. Luzon, C. Degl’Innocenti, M. Perfetti, K. Bernot, G. Calvez, A. Caneschi and R. Sessoli, *Angew. Chem., Int. Ed.*, 2013, **52**, 350; (b) G. Cucinotta, M. Perfetti, J. Luzon, M. Etienne, P.-E. Car, A. Caneschi, G. Calvez, K. Bernot and R. Sessoli, *Angew. Chem., Int. Ed.*, 2012, **51**, 1606; (c) F. Pointillart, B. L. Guennic, S. Golhen, O. Cador, O. Maury and L. Ouahab, *Chem. Commun.*, 2013, **49**, 615; (d) A. B. Canaj,

- D. I. Tzimopoulos, A. Philippidis, G. E. Kostakis and C. J. Milios, *Inorg. Chem.*, 2012, **51**, 7451; (e) D. I. Alexandropoulos, S. Mukherjee, C. Papatriantafyllopoulou, C. P. Raptopoulou, V. Psycharis, V. Bekiari, G. Christou and Th. C. Stamatatos, *Inorg. Chem.*, 2011, **50**, 11276; (f) M. Menelaou, F. Ouharrou, L. Rodríguez, O. Roubeau, S. J. Teat and N. Aliaga-Alcalde, *Chem.-Eur. J.*, 2012, **18**, 11545; (g) K. Yamashita, R. Miyazaki, Y. Kataoka, T. Nakanishi, Y. Hasegawa, M. Nakano, T. Yamamura and T. Kajiwara, *Dalton Trans.*, 2013, **42**, 1987; (h) C. E. Burrow, T. J. Burchell, P.-H. Lin, F. Habib, W. Wernsdorfer, R. Clérac and M. Murugesu, *Inorg. Chem.*, 2009, **48**, 8051.
- 17 D. N. Woodruff, R. E. P. Winpenny and R. A. Layfield, *Chem. Rev.*, 2013, **113**, 5110.
- 18 (a) S. V. Eliseeva and J.-C. Bünzli, *New J. Chem.*, 2011, **35**, 1165; (b) M. D. Ward, *Coord. Chem. Rev.*, 2010, **254**, 2634; (c) T. Förster, *Chem. Phys. Lett.*, 1971, **12**, 422.
- 19 P. D. Fleischauer and P. Fleischauer, *Chem. Rev.*, 1970, **70**, 199, and references cited therein.
- 20 Th. C. Stamatatos, D. Foguet-Albiol, C. C. Stoumpos, C. P. Raptopoulou, A. Terzis, W. Wernsdorfer, S. P. Perlepes and G. Christou, *J. Am. Chem. Soc.*, 2005, **127**, 15380.
- 21 (a) S. L. Williams, I. Kirkpatrick and D. R. Worrall, *Photochem. Photobiol. Sci.*, 2010, **9**, 937; (b) B. L. Feringa, *Molecular Switches*, Wiley-VCH, 2001; (c) A. P. Demchenko, *Introduction to Fluorescence Sensing*, Springer, 2009.
- 22 Anal. calcd (found) for 2–4 (all solvent-free): C 54.08 (54.37), H 3.53 (3.62), N 7.01 (6.76); C 58.75 (58.82), H 3.59 (3.71), N 6.23 (6.02); C 60.84 (60.95), H 3.40 (3.47), N 5.91 (5.85). Crystal structure data for 2:  $C_{132}H_{78}Mn_6N_{12}O_{32}Cl_3$ ,  $M_w = 2780.06$ , monoclinic, space group  $P2_1/c$  with  $a = 20.223(5)$ ,  $b = 18.555(5)$ ,  $c = 19.641(5)$  Å,  $\beta = 118.303(10)^\circ$ ,  $V = 6489(3)$  Å<sup>3</sup>,  $T = 150(2)$  K,  $Z = 4$ ,  $R1 [I > 2\sigma(I)] = 0.0738$ ,  $wR2 = 0.1675 (F^2, \text{all data})$ . Crystal structure data for 3:  $C_{66}H_{48}Mn_3N_6O_{14}Cl$ ,  $M_w = 1349.42$ , trigonal, space group  $P\bar{3}c1$  with  $a = b = 18.4788(10)$ ,  $c = 28.5885$  Å,  $V = 8454.1(10)$  Å<sup>3</sup>,  $T = 150(2)$  K,  $Z = 2$ ,  $R1 [I > 2\sigma(I)] = 0.0926$ ,  $wR2 = 0.2748 (F^2, \text{all data})$ .
- 23 N. E. Chakov, S.-C. Lee, A. G. Harter, P. L. Kuhns, A. Reyes, S. O. Hill, N. S. Dalal, W. Wernsdorfer, K. A. Abboud and G. Christou, *J. Am. Chem. Soc.*, 2006, **128**, 6975.
- 24 J. Cano, T. Cauchy, E. Ruiz, C. J. Milios, C. C. Stoumpos, Th. C. Stamatatos, S. P. Perlepes, G. Christou and E. K. Brechin, *Dalton Trans.*, 2008, 234.
- 25 (a) A. D. Katsenis, R. Inglis, A. Prescimone, E. K. Brechin and G. S. Papaefstathiou, *CrystEngComm*, 2012, **14**, 1216; (b) R. Inglis, S. M. Taylor, L. F. Jones, G. S. Papaefstathiou, S. P. Perlepes, S. Datta, S. Hill, W. Wernsdorfer and E. K. Brechin, *Dalton Trans.*, 2009, 9157.
- 26 (a) F. P. Schawrz and S. P. Wasik, *Anal. Chem.*, 1976, **48**, 524; (b) K. Uchida and Y. Takahashi, *Int. J. Quantum Chem.*, 1980, **18**, 301.